

The Evolution of Galactic Disks

Shude Mao, H.J. Mo and Simon D.M. White [★]

Max-Planck-Institut für Astrophysik Karl-Schwarzschild-Strasse 1, 85748 Garching, Germany

Accepted Received; in original form

ABSTRACT

We use recent observations of high-redshift galaxies to study the evolution of galactic disks over the redshift range $0 < z \lesssim 1$. The data are inconsistent with models in which disks were already assembled at $z = 1$ and have evolved only in luminosity since that time. Assuming that disk properties change with redshift as powers of $1 + z$ and analysing the observations assuming an Einstein-de Sitter universe, we find that for given rotation speed, disk scalelength decreases with z as $\sim (1 + z)^{-1}$, total B -band mass-to-light ratio decreases with z as $\sim (1 + z)^{-1}$, and disk luminosity (again in B) depends only weakly on z . These scalings are consistent with current data on the evolution of disk galaxy abundance as a function of size and luminosity. Both the scalings and the abundance evolution are close to the predictions of hierarchical models for galaxy formation. If different cosmogonies are compared, the observed evolution in disk-size and disk abundance favours a flat low- Ω_0 universe over an Einstein-de Sitter universe.

Key words: galaxies: formation - galaxies: evolution - galaxies: spirals - cosmology: theory - dark matter

1 INTRODUCTION

The Hubble Space Telescope (HST) and large ground-based telescopes can now provide photometric and kinematic data for normal galaxies out to redshifts of about one. Such observations are providing new results on the evolution of disk galaxies, showing that the population of these objects changes substantially with cosmic time. For example, disks of a

[★] E-mail: (smao, hom, swhite)@mpa-garching.mpg.de

given size appear brighter in the past, or equivalently disks of given luminosity appear smaller (e.g. Schade et al 1996; Lilly et al 1997 and references therein). A traditional approach to interpreting such data has invoked luminosity evolution, assuming that normal giant galaxies were already assembled by redshift unity and have evolved primarily in luminosity since that time. The purpose of this paper is to examine this hypothesis in the light of recent data on disk sizes, luminosities and kinematics. We find it to be untenable if the data are taken at face value; strong evolution in the structure of disks appears to be required. The form of this evolution is quite similar to that expected in recent models for disk formation in hierarchical cosmologies.

In §2, we use recent local and high-redshift galaxy samples to fit for the values of the exponents in power-law representations of the evolution of disk sizes, luminosities, rotation speeds and abundances. In §3, we derive the scaling relations predicted for disk properties by hierarchical models and we compare them with the observational relations. §4 presents some discussion of these results.

To avoid confusion, we transform all cosmology-dependent observational quantities to an assumed Einstein-de Sitter (EdS) universe with $h = 0.5$ (where h is the present Hubble constant in units of $100 \text{ km s}^{-1} \text{ Mpc}^{-1}$). We transform theoretical predictions in this way also, even when they refer to a different cosmology.

2 OBSERVATIONAL FACTS

To study the photometric and kinematic evolution of galaxies, we obviously need both high-redshift and local samples. For the high-redshift data, we use primarily the Canada-France Redshift Survey (hereafter CFRS, see Lilly et al 1995; Schade et al 1996) and the KECK kinematical study of Vogt et al (1997a,b). Ideally, we would like to have a local galaxy sample that has both photometric and kinematic information. However, at present this is not yet available. We therefore make use of several samples (Kent 1985; Pierce & Tully 1988, 1992; Courteau 1996, 1997; de Jong & van der Kruit 1994, de Jong 1996). We use simple power-law parametrisations of the evolution of observational relations (size-rotation speed, size-luminosity, abundance-luminosity, Tully-Fisher, etc.) and we determine the evolution exponents *empirically* from the data.

2.1 The R_d - V_c Relation

We first study the relation between disk size and rotation speed. The local sample is from Courteau (1996, 1997) whereas the high-redshift data are taken from Vogt et al (1997a,b). There are respectively 306 and 16 galaxies in these two samples. Figure 1a shows the histogram of $\log Q_{rv} \equiv \log R_d/V_c$, where R_d (in kpc) is the disk scale-length and V_c (in km s^{-1}) is the rotation speed. The R_d distribution at fixed V_c is expected to scale in proportion to V_c with a coefficient depending on the redshift (see §3); the marginal distribution of R_d/V_c should thus isolate the redshift dependence clearly. The dashed line is for the high-redshift data while the solid line is for the local sample. Clearly R_d/V_c is smaller at high-redshift, i.e., for given V_c , high-redshift disks are smaller (Vogt et al 1997a,b). According to a Kolmogorov-Smirnov (KS) test, the probability that these two samples are drawn from the same parent distribution is 1.5×10^{-4} . Clearly the assumption that disk sizes have not changed since $z = 1$ is inconsistent with the data. This excludes models with pure luminosity evolution. To quantify the size evolution, we adopt simple parametrisation, $Q_{rv}(z) = Q_{rv}(0)(1+z)^{\beta_{rv}}$, and evolve each high-redshift galaxy to the present day. We then compare the evolved distribution of R_d/V_c to that of the local sample using the KS test. The resulting probability is shown as the solid line in Figure 1d. One can see that the most probable value of β_{rv} (corresponding to the largest KS probability) is $\beta_{rv} = -0.95$, with values outside $-1.4 < \beta_{rv} < -0.54$ excluded at 95% confidence.

2.2 The Tully-Fisher Relation

Vogt et al (1997a,b) have studied the evolution of the Tully-Fisher relation with redshift. They obtained kinematic data for high- z disks using KECK spectroscopy and compared them to the local B -band Tully-Fisher relation of Pierce & Tully (1988, 1992). We have converted their quoted data to correspond to an assumed EdS cosmology with $h = 0.5$ (see §3). Unlike the R_d - V_c relation discussed above, the comparison between the high- and low-redshift Tully-Fisher relations suffers from the uncertainties in the relative calibration of the various photometric systems. We follow Vogt et al in comparing to the Pierce & Tully sample even though it contains only 26 galaxies in the Ursa Major cluster, but we note that the Tully-Fisher zero-point of this cluster has a significant systematic uncertainty (c.f. Giovanelli et al 1997). We define the quantity $Q_{tf} \equiv L/V_c^3$, where L denotes galaxy luminosity. Since L is roughly proportional to V_c^3 , the distribution of Q_{tf} can be used to measure evolution of

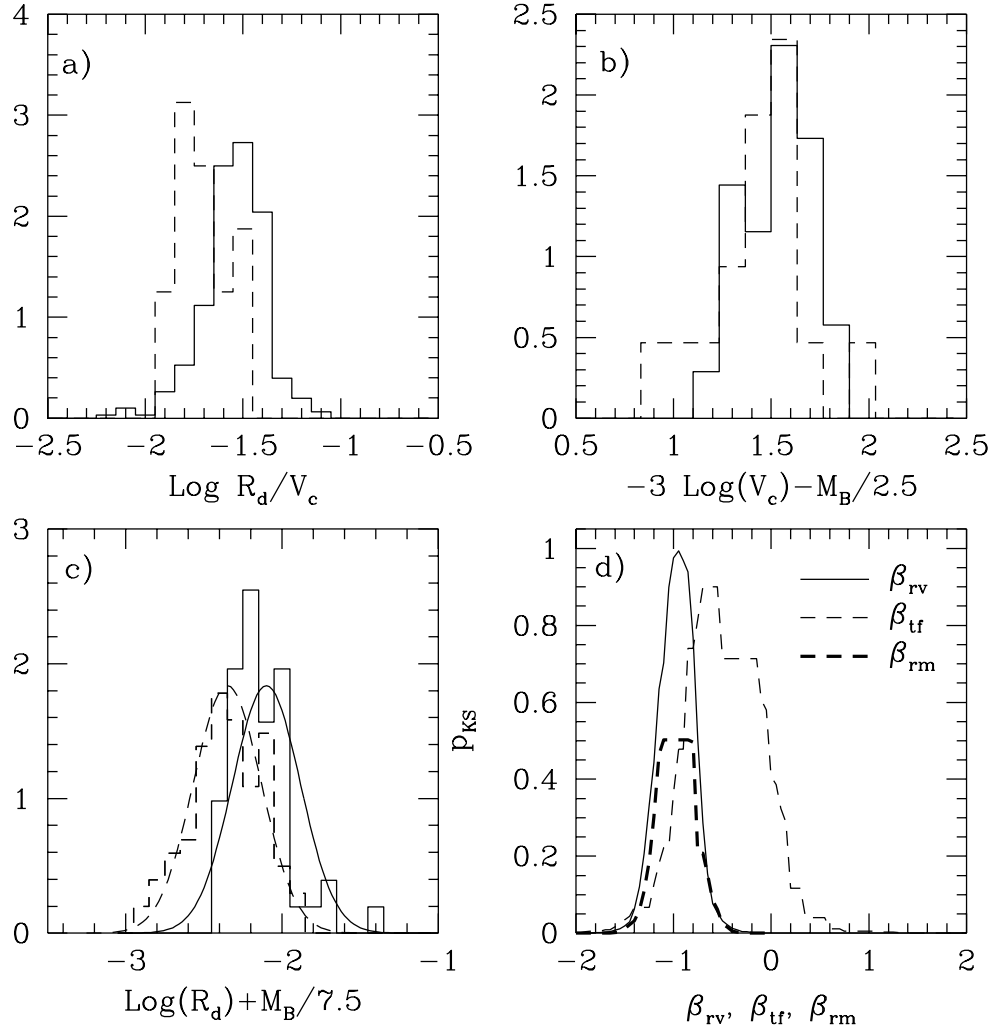


Figure 1. Histograms for various physical quantities for local (solid lines) and high-redshift (dashed lines) samples. The area under all the histograms is one. (a) $\log Q_{rv} \equiv \log R_d/V_c$. The local sample is from Courteau (1996, 1997) and has 306 galaxies. The high-redshift sample from Vogt et al (1997a,b) has 16 galaxies. (b) $\log Q_{tf} \equiv -3 \log(V_c) - M_B/2.5$. The local sample is from Pierce & Tully (1988) and has 26 galaxies. The high-redshift sample is the same as in Fig. 1a. (c) $\log Q_{rm} \equiv \log(R_d) + M_B/7.5$. The local r -band sample is from Kent (1985) and has 51 galaxies. We have converted it to B using $B - r = 0.9$ (Kent 1984). The high-redshift sample from the CFRS survey (Schade et al 1996) has 103 galaxies. The solid and dashed curves are normal fits to the local and high-redshift data. (d) KS test probability as a function of evolution exponents for the three physical quantities plotted in panels a, b and c (see text).

the zero-point of the Tully-Fisher relation. Histograms of $\log Q_{tf} = -M_B/2.5 - 3 \log V_c$ are shown in Fig. 1b. Here M_B is the B-band absolute magnitude of the galaxies. It is clear that the data are consistent with no zero-point evolution, in agreement with the conclusion of Vogt et al (1997a,b) and Hudson et al (1997). A KS test shows the no-evolution assumption to be acceptable. To put limits on evolution of the Tully-Fisher relation, we set $Q_{tf}(z) = Q_{tf}(0)(1+z)^{\beta_{tf}}$ and perform KS tests on the “evolved” distributions as before. The constraints

on β_{tf} are indicated by the thin dashed line in Figure 1d. With the current data, the evolution index is not well constrained, only values outside $-1.44 < \beta_{\text{tf}} < 0.36$ can be excluded with better than 95% confidence. More data, particularly at high-redshift, are needed to tie down the evolution of Tully-Fisher relation, and it is important to ensure consistent photometric systems at high- and low-redshift. If we combine the R_d - V_c and Tully-Fisher relations, we can estimate the evolution of the total B -band mass-to-light ratio of the visible regions of galaxies: $M/L \propto V_c^2 R_d / L = Q_{\text{rv}} / Q_{\text{tf}} \propto (1+z)^{\beta_{\text{rv}} - \beta_{\text{tf}}}$. For $\beta_{\text{tf}} = 0$, this gives $M/L \propto (1+z)^{-1.0}$. However, if the most likely value of β_{tf} is used, then $M/L \propto (1+z)^{-0.5}$. The exponent here is quite uncertain as a result of the uncertain evolution of the Tully-Fisher relation.

2.3 The R_d - M_B Relation

Next we examine the evolution of R_d - M_B relation. We compare the local (volume-limited) sample of Kent (1985) with the high-redshift data of Schade et al (1996). We have checked that the independent local (diameter-limited) sample of de Jong (1996) roughly agrees with that of Kent, when the different selection functions are properly taken into account. Figure 1c shows histograms of the quantity $\log Q_{\text{rm}} \equiv \log(R_d) + M_B/7.5$ for the local and high-redshift samples. Notice that for a tight Tully-Fisher relation of the form $L \propto V_c^3$, Q_{rm} should be distributed similarly at each redshift to the Q_{rv} discussed in §2.1. For a no-evolution model, the high- and low-redshift histograms would coincide. Instead, one clearly sees that disks of given luminosity are smaller at earlier times, or equivalently, galaxies of given size are brighter. A KS test reveals that the probability that these two samples are drawn from the same distribution is less than 4.9×10^{-6} . Parametrising evolution of the size-luminosity relation as $Q_{\text{rm}}(z) = Q_{\text{rm}}(0)(1+z)^{\beta_{\text{rm}}}$, we estimate β_{rm} as before using a KS test. The result is shown by the thick dashed line in Figure 1d. The most probable value is $\beta_{\text{rm}} = -1.0$ and values outside $-1.35 < \beta_{\text{rm}} < -0.53$ can be excluded with 95% significance. This result agrees with Schade et al (1996) who found that the luminosity of disks of given size increases approximately as $(1+z)^3$ in the CFRS. If we use only the big disks as defined in Lilly et al (1997), then we obtain $\beta_{\text{rm}} \sim -0.5$. This indicates that there might be some differential evolution in the $R_d - M_B$ relation for small and big disks. Unfortunately, current data do not allow a more detailed analysis of this evolution.

2.4 Disk Size Functions

Schade et al (1996) studied the redshift dependence of the abundance of disk galaxies as a function of size. By analogy with the luminosity function this quantity is referred to as the “size function”. They found that the abundance of big, bright disks (scalelengths larger than 5 kpc and absolute magnitudes brighter than -20) is similar at $z \sim 0.3$ and at 0.75, whereas the abundance of small, bright disks (scalelengths less than 4 kpc but $M_B < -20$) is 5 – 10 times higher at the higher redshift. A comparison of more recent HST imaging of CFRS and LDSS galaxies with the local sample of De Jong et al (1996) confirms and strengthens this result (Lilly et al 1997). In addition, if all galaxies to the CFRS limit are included, the size functions for low- and high-redshift samples are similar. These authors interpret their results as suggesting that the abundances and sizes of big disks have not changed significantly since $z = 1$; the observed evolution reflects changes in disk luminosity caused by changes in star formation rate. This interpretation conflicts with our earlier conclusions, and in this subsection we test whether the observed size functions are also consistent with evolution of the kind inferred above.

We start with the observed luminosity functions for disk galaxies at various redshifts. Using an empirical Gaussian fit to the distributions of $\log(R_d) + M_B/7.5$ in Fig. 1c, and assuming that for given M_B disk size varies as $R_d \propto (1+z)^{-1}$ (see §2.3), we can transform the luminosity function into a size function at each redshift. The solid curves in Figure 2 show the size functions derived from the luminosity functions given by Lilly et al (1995) for blue galaxies (which are mostly late-type galaxies) in the CFRS. Results are shown for two absolute magnitude limits $M_B = -20$ and $M_B = -18.5$: the former is approximately the magnitude limit for the high-redshift sample (with median redshift 0.75) whereas the latter is that for the low-redshift sample (with median redshift 0.3). We see that the abundance of disks with $R_d > 4$ kpc hardly changes with redshift while the abundance of smaller galaxies changes substantially. Not surprisingly, this agrees well with the conclusions of Schade et al (1996) and Lilly et al (1997) since both our evolution rate and our distribution of R_d for given M_B were derived from the CFRS data.

We now compare these size functions with a model based on the kind of evolution inferred in previous sections. Let us approximate the (comoving) abundance of galaxies with rotation speed V_c at redshift z as

$$N(V_c, z)dV_c = N_\star(1+z)^{\beta_n} \left(\frac{V_c}{V_\star}\right)^\gamma \frac{dV_c}{V_\star}, \quad (1)$$

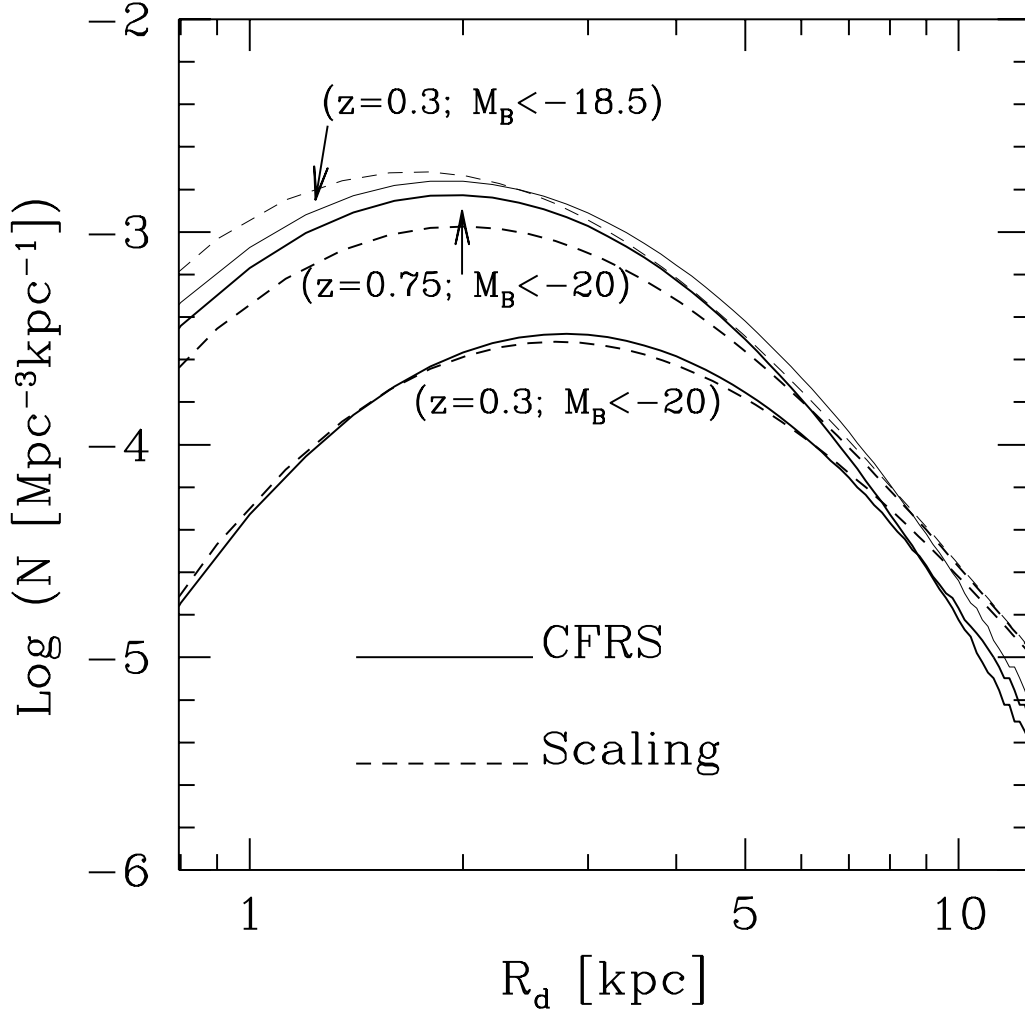


Figure 2. The size functions for galactic disks. The solid curves show results derived directly from the CFRS, whereas the dashed curves show the model of equation (3) for $\beta_{rv} = -1.0$, $\beta_n = 3.0$, $\gamma = -4$ and $N_\star = 1.0 \times 10^{-3} \text{Mpc}^{-3}$. The lower pair of curves is for galaxies with $M_B < -20$ at $z = 0.3$; the middle pair for galaxies with $M_B < -20$ at $z = 0.75$; the upper pair for galaxies with $M_B < -18.5$ at $z = 0.3$.

where V_\star is some fiducial rotation speed, N_\star is the abundance of V_\star galaxies, β_n parameterises the abundance evolution, and γ parameterises the shape of the rotation speed function. Note that this is a *minimal* parametrisation, which can be valid only over limited ranges of V_c and z . In practice we are interested in values of V_c similar to those of L_\star galaxies. If, as observations suggest, disks show a reasonably tight Tully-Fisher relation at each redshift, we can use the parametrisation of §2.2 to convert this to a luminosity function,

$$N(L, z)dL = \frac{1}{3}N_\star(1+z)^{\beta_n} \left(\frac{L}{L_\star(z)} \right)^{(\gamma-2)/3} \frac{dL}{L_\star(z)} \propto (1+z)^{\beta_n-(\gamma+1)\beta_{tf}/3} L^{(\gamma-2)/3} dL, \quad (2)$$

where $L_*(z) = (1+z)^{\beta_{\text{tf}}} L_{*,0}$ and $L_{*,0}$ is the luminosity corresponding to V_* at $z = 0$.

In §2.1 we found that the mean size-rotation speed relation can be well represented by $R_d \propto V_c(1+z)^{\beta_{\text{rv}}}$. The scatter in $\ln R_d$ about this relation is approximately normal with an *rms* of $\sigma \approx 0.5$ (cf. Fig. 1c). This allows us to calculate the size function for galaxies with absolute B -magnitude brighter than M_{lim} and so rotation speed greater than $(L_{\text{lim}}/L_*)^{1/3} V_*$. We find

$$N(R_d, z) dR_d = N_*(1+z)^{\beta_n} \left[\frac{R_d}{R_*(z)} \right]^\gamma \frac{dR_d}{R_*(z)} \times \int_{-\infty}^{x_{\text{max}}} \frac{1}{\sqrt{2\pi}\sigma} \exp \left[-\frac{x^2}{2\sigma^2} - (1+\gamma)x \right] dx; \quad (3)$$

$$x_{\text{max}} = [\ln(10)/7.5] (M_{\text{lim}} - M_*) + \ln[R_d/R_*(z)], \quad (4)$$

where M_* is the absolute magnitude corresponding to L_* , and $R_*(z) = R_0(1+z)^{\beta_{\text{rv}}}$ is the median value of disk scalelength for galaxies with $V_c = V_*$ at redshift z . From the solid histogram shown in Fig. 1a we have $(R_0/\text{kpc}) \approx 0.03(V_*/\text{km s}^{-1})$. For $M_{\text{lim}} \gtrsim M_*$ and $R_d \gg R_*(z)$, the integration in equation (3) depends only weakly on R_d , and the size function scales with R_d and z as

$$N(R_d, z) dR_d \propto (1+z)^{\beta_n - (1+\gamma)\beta_{\text{rv}}} R_d^\gamma dR_d. \quad (5)$$

Thus, the observational result that the comoving number density of large and bright disks does not change significantly with redshift requires $\beta_n \sim \beta_{\text{rv}}(1+\gamma)$.

The interpretation of Schade et al (1996) and Lilly et al (1997) corresponds to $\beta_n = \beta_{\text{rv}} = 0$ and $\beta_{\text{tf}} = 3$ – no evolution in abundance or size but strong evolution in luminosity. In contrast, our earlier analysis suggested $\beta_{\text{rv}} \sim -1$, implying $\beta_n \sim -(1+\gamma)$. At luminosities around L_* the slope of observed luminosity functions is near -2 which, according to equation (2), corresponds to $\gamma \sim -4$. Consistency then requires $\beta_n \sim 3$. In Fig. 2 we show the predictions of equation (3) for $\beta_{\text{rv}} = -1.0$, $\beta_n = 3.0$, $\gamma = -4$, $N_* = 1.0 \times 10^{-3} \text{Mpc}^{-3}$ and $M_{\text{lim}} = -20$. These agree well both with the size functions derived from the luminosity functions of Lilly et al (1995) and with the direct observational estimates of Schade et al (1996). The figure also shows predictions for disks at $z = 0.3$ with $M_B < -18.5$. The size function of this low-redshift sample is similar to that of the high-redshift sample limited at $M_B = -20$ as found by Lilly et al (1997) in their observational samples. We conclude that the observed size functions are indeed compatible with a model in which disks of given rotation speed have a size which varies as $(1+z)^{-1}$ and an abundance which varies as $(1+z)^3$. If the redshift dependence of the Tully-Fisher relation is weak, then at fixed luminosity the

comoving density in this model evolves approximately as $(1+z)^3$ (see equation [2]). This agrees with the behaviour which Lilly et al (1996) inferred from an analysis of the comoving B -band luminosity density.

3 MODEL SCALINGS

The analysis of the last section shows that current data are inconsistent with the hypothesis that disk galaxies were already assembled at redshift unity and have only evolved in luminosity since that time. The current section compares with the predictions of hierarchical models for galaxy formation, based on the work reported in Mo, Mao & White (1997). To clarify the relevant scalings, it is sufficient to treat galaxies as exponential disks embedded in isothermal halos; for simplicity we neglect both the disk mass and the halo core radius. The luminosity and size of the disk then scale as

$$L \propto \frac{1}{\Upsilon_{\text{tot}}(z)} V_c^3 \frac{H_0}{H(z)}, \quad R_d \propto \lambda \frac{V_c}{H_0} \frac{H_0}{H(z)}, \quad (6)$$

where Υ_{tot} is the total mass-to-light ratio within the *halo virial radius* and λ is the dimensionless spin parameter. For given circular velocity, disk size depends on redshift only through the Hubble constant $H(z)$, while the luminosity has an additional dependence through the mass-to-light ratio. If we make the approximations $\Upsilon_{\text{tot}}(z) = \Upsilon_{\text{tot}}(0)(1+z)^{\beta_r}$ and $H(z) = H_0(1+z)^{\beta_h}$, then from the definitions, $Q_{\text{tf}} \equiv L/V_c^3$ and $Q_{\text{rv}} \equiv R_d/V_c$, we have

$$Q_{\text{tf}}(z) = Q_{\text{tf}}(0)(1+z)^{-\beta_r-\beta_h}, \quad Q_{\text{rv}}(z) = Q_{\text{rv}}(0)(1+z)^{-\beta_h}. \quad (7)$$

Thus we see that β_h is equal to β_{rv} as defined above. In an EdS universe, $\beta_h = 3/2$, so this simple model predicts that for given circular velocity, the mean size of disks should vary as $(1+z)^{-3/2}$. This is somewhat too steep to be compatible with the data analysed in §2.1 (cf. Figure 1d).

In order to compare the data with predictions for other cosmologies, we can either reanalyse the observations assuming the cosmology under consideration, or transform the model predictions into those expected when the data are analysed *assuming* an EdS universe. Here we adopt the second approach. Cosmology enters our problem through the Hubble constant, the angular size and luminosity distances and the comoving volume. For moderate redshifts ($0 < z < 1$), the ratios of these quantities in a general cosmology to those in an EdS universe can be approximated by power-laws in $1+z$:

$$\frac{\widetilde{H}(z)}{H(z)} = (1+z)^{\alpha_h}, \quad \frac{\widetilde{d_A}(z)}{d_A(z)} = (1+z)^{\alpha_d}, \quad \frac{\widetilde{dv/dz}}{dv/dz} = (1+z)^{\alpha_v}, \quad (8)$$

where the tilded quantities refer to the EdS cosmology; d_A is the angular diameter distance and dv/dz is the differential comoving volume. The indices α_h, α_d and α_v can be approximated by

$$\alpha_h = -1.5(1 - \Omega_0^{0.90}), \quad \alpha_d = 0.78(1 - \Omega_0^{0.67}), \quad \alpha_v = 3.1(1 - \Omega_0^{0.65}), \quad (9)$$

for flat cosmologies with $\Omega_0 + \Lambda = 1$, and by

$$\alpha_h = -0.5(1 - \Omega_0^{0.65}), \quad \alpha_d = 0.35(1 - \Omega_0^{0.90}), \quad \alpha_v = 1.2(1 - \Omega_0^{0.80}), \quad (10)$$

for open cosmologies with $\Omega_0 \leq 1$ and $\Lambda = 0$. Using the definitions of Q_{rv} , Q_{rm} and Q_{tf} together with equations (6) and (8) we have

$$\beta_{rv} = -\alpha_d - \alpha_h - \frac{3}{2}, \quad \beta_{tf} = -2\alpha_d - \alpha_h - \beta_{\Upsilon} - \frac{3}{2}, \quad \beta_{rm} = \beta_{rv} - \frac{\beta_{tf}}{3}. \quad (11)$$

These allow the predicted evolution exponents for any cosmological model to be compared directly with the observed exponents estimated assuming an EdS universe. For example, a flat cosmology with $\Omega_0 = 0.3$ and $\Lambda = 0.7$ has $\alpha_h = -1.0$, $\alpha_d = 0.43$ and $\alpha_v = 1.68$. Hence $\beta_{rv} = -0.93$ and $\beta_{tf} = -1.36 - \beta_{\Upsilon}$. If there is no evolution in the Tully-Fisher zero-point (cf. §2.2), then $\beta_{\Upsilon} = -1.36$, and $\beta_{rm} = -0.93$, in reasonable agreement with the exponents inferred from the data in §2.

The values of β_n and γ characterizing the number-density evolution of disks (cf. equation [1]) can be estimated from the Press-Schechter formalism (Press & Schechter 1974). This provides simple formulae for the comoving abundance of haloes as a function of redshift and of halo mass M_h or circular velocity V_c (e.g. White & Frenk 1991). For currently popular cosmogonies, the slope of the abundance curves for V_c values corresponding to the rotation speeds of observed disks implies $\gamma \sim -3.5 \rightarrow -3.8$, while the evolution of the abundance at fixed V_c in this range gives $\beta_n \sim 1.3 \rightarrow 1.7$ for CDM-like models with $\Omega_0 = 1$ and $\beta_n \sim 2.9 \rightarrow 3.3$ for a flat model with $\Omega_0 = 0.3$ and $\Lambda = 0.7$. The larger β_n in the latter model is due to the volume correction to the EdS universe (cf. equation 9). These values are quite similar to those inferred empirically in §2, particularly for the flat model with low Ω_0 . Thus the observed evolution both in abundance and in systematic parameter relations seems compatible with the expectations of hierarchical formation theories.

4 DISCUSSION

We have shown that current data appear inconsistent with models in which disk galaxies are already assembled by redshift one and have evolved only in luminosity since that time. Assuming that disk properties vary as powers of $1 + z$ and analysing them under the assumption of an EdS universe, we find that for given rotation speed, disk scalelength varies as $\sim (1 + z)^{-1}$, total mass-to-light ratio (in the B -band) as $\sim (1 + z)^{-1}$, disk luminosity (in B -band) is almost independent of z , and disk abundance varies as $\sim (1 + z)^3$. These scalings agree well with the predictions of hierarchical models for flat low-density universes but are marginally weaker than expected in an Einstein-de Sitter universe. Our results for the evolution of the size, luminosity and abundance of disk galaxies can be compared to those of Bouwens, Broadhurst & Silk (1997) who modeled the counts of faint galaxies as a function of apparent magnitude, colour and size in the Hubble Deep Field (Williams et al 1996). Their preferred model corresponds to $\beta_n \sim 3.5$ and $\beta_{rm} \sim -1.5$, similar to the values derived here.

In the tests described in this paper, our own preferred model is distinguished from the simpler hypothesis proposed by Schade et al (1996) and Lilly et al (1997) only because we have included kinematic data. Our results therefore depend critically on the high-redshift observations of Vogt et al (1997a,b). The apparent evolution of the size-rotation speed relation is inconsistent with pure luminosity evolution, which also requires stronger luminosity evolution than can be reconciled with the weak redshift-dependence of the Tully-Fisher relation. The Vogt et al sample is quite small and the comparison of its Tully-Fisher zero-point to that of local samples is uncertain. Further kinematic and photometric data for high-redshift galaxies are necessary to confirm the conclusions we have reached. Only with the inclusion of kinematic information is it easy to separate evolution in the mass and size of galaxies from evolution in their stellar mass-to-light ratio.

ACKNOWLEDGMENTS

We are grateful to Nicole Vogt and Stephane Courteau for providing us data in electronic form. This project is partly supported by the ‘‘Sonderforschungsbereich 375-95 für Astro-Teilchenphysik’’ der Deutschen Forschungsgemeinschaft.

REFERENCES

- Bouwens R., Broadhurst T., Silk J. 1997, ApJ, submitted (astro-ph/9710291)
- Courteau S., 1996, ApJS, 103, 363.
- Courteau S., 1997, ApJS, in press.
- de Jong R.S., van der Kruit P.C., 1994, A&AS, 107, 419
- de Jong R.S., 1996, A&AS, 118, 557
- Ellis R.S., Colless M., Broadhurst T., Heyl J. & Glazebrook K. 1996, MNRAS, 280, 235
- Giovanelli R., Haynes M.P., Herter T., Vogt N.P., da Costa L.N., Freudling W., Salzer J.J., 1997, AJ, 113, 53
- Hudson M.J., Gwyn S.D.J., Dahle H., Kaiser N., 1997, ApJ, submitted (astro-ph/9711341)
- Kent S., 1984, ApJS, 56, 105
- Kent S., 1985, ApJS, 59, 115
- Lilly S.J., Tresse L., Hammer F., Crampton D., & Le Fevre O. 1995, 455, 108
- Lilly S.J., Le Fevre O., Hammer F., & Crampton D. 1996, 460, L1
- Lilly S.J., Schade D., Ellis R.S., Le Fevre O., Brinchmann J., Abraham, A., Tresse L., Hammer F., Crampton D., Colless M., Glazebrook K., Mallen-Ornelas G., Broadhurst T. 1997, preprint (astro-ph/9712061)
- Mo H.J., Mao S., & White S.D.M., 1997, MNRAS, in press (astro-ph/9707093)
- Pierce M.J., & Tully B.R. 1988, 330, 579
- Pierce M.J., & Tully B.R. 1992, 387, 47
- Press W.H., Schechter P., 1974, ApJ, 187, 425
- Schade D., Lilly S.J., Le Fevre O., Hammer F., Crampton D., 1996, 464, 79
- Vogt N.P., Forbes D. A., Phillips A.C., Gronwall C., Faber S.M., Illingworth G.D., Koo D., 1997a, ApJ, 465, L15
- Vogt N.P., Phillips A.C., Faber S.M., Gallego J., Gronwall C., Guzmàn R., Illingworth G.D., Koo D., & Lowenthal J.D., 1997b, ApJ, 479, L121
- White S.D.M., Frenk C.S., 1991, ApJ, 379, 52
- Williams R.E., et al 1996, AJ, 112, 1335

This paper has been produced using the Royal Astronomical Society/Blackwell Science L^AT_EX style file.